Comments® on
PLASMA PHYSICS AND CONTROLLED FUSION

CONTENTS Vol. XII, No. 2 (1988)

Conference Report

Comments® on Plasma Physics and Controlled Fusion

A Journal of Critical Discussion of the Current Literature

Comments on Modern Physics: Part E

Volume XII
Number 3(1989)

CPCFBJ 12(3) 113–170(1989)
ISSN 0374-2806

4. P. Rosenau, Phys. Fluids **22**, 249 (1979).
5. S. V. Bulanov and M. A. Ol'shanetskij, Phys. Lett. **100A**, 35 (1984).
6. S. V. Bulanov and M. A. Ol'shanetskij, Fiz. Plazmy **11**, 727 (1985) [Sov. J. Plasma Phys. **11**, 425 (1985)].
7. S. V. Bulanov, I. Ya. Butov, Yu. S. Gvaladze *et al.*, Fiz. Plazmy **12**, 309 (1986) [Sov. J. Plasma Phys. **12**, 180 (1986)].
8. J. W. Dungey, Philosoph. Mag. **44**, 725 (1953).
9. V. S. Imshennik and S. I. Syrovatskij, Zh. Eksp. Teo. Fiz. **52**, 990 (1967) [Sov. Phys.-JETP **25**, 656 (1967)].

Maximum *J* Tokamak by Plasma Shaping

Plasma stability to trapped particle modes in the regime $\nu_* < 1$ is improved by plasma shaping. Using numerically generated equilibria the single particle drift frequency ω_d is calculated from the derivative of the second adiabatic invariant J. Reversal of the single particle drifts, averaged over the trapped particle population for a range of flux surfaces is achieved through shape optimization at $\beta = 0$. The optimal shape found has a very small aspect ratio, $R/a = 1.25$. The plasma cross-section is "comet-shaped" with the tip of the tail pointed towards the major axis.

Key Words: *tokamak, maximum J, trapped particles, transport, confinement, non-circular*

Recently, Ohkawa[1] has made the suggestion of using plasma shaping to improve plasma confinement in tokamaks. Although great emphasis has been placed on plasma shaping to improve the stable plasma beta limit,[2-4] relatively little has been done with regard to plasma shaping for improved confinement.

Here we concentrate on mitigating the effects of the trapped particle modes by improving the single particle drift orbits through plasma shaping. This geometric approach can achieve drift reversal ($\omega_* \omega_d < 0$) even at $\beta = 0$, in contrast to a diamagnetic approach. The latter requires significant β where electromagnetic effects become important and other instabilities may arise. There is evidence that trapped particle modes were seen in the spherator and that they were stabilized by changing the magnetic geometry so that the trapped particles were in a good curvature region.[5]

Comments Plasma Phys. Controlled Fusion
1989, Vol. 12, No. 3, pp. 125–132
Reprints available directly from the publisher
Photocopying permitted by license only

At the extreme case of $\nu_* = 0$, the stability of the collisionless trapped particle mode is completely determined by the single particle drifts, ω_d. In this limit the effect of plasma shaping, primarily elongation, has been previously considered[6,7] and found to lead to drift reversal only for large elongation and $\beta_p \gtrsim 1$. Here β_p is the ratio of the plasma pressure to the poloidal magnetic field pressure. Tang[8] has considered the effect of toroidal drifts on the dissipative trapped ion mode and found significant stabilization for large elongation and $\beta_p = 1$.

The effect of reversing the single particle drift, ω_d, is strongest for the collisionless trapped particle mode where it determines stability,[9]

$$\frac{\partial J}{\partial \psi}\frac{\partial p}{\partial \psi} > 0. \tag{1}$$

Here J is the second adiabatic invariant,

$$J = \oint v_{\|} dl, \tag{2}$$

p is the plasma pressure, ψ the poloidal flux, dl a line element along the field line, and $v_{\|}$ is the velocity parallel to the magnetic field. The bounce-averaged particle drift in the toroidal direction can be obtained from

$$\omega_d = \frac{\Delta\phi}{\tau_b} = \frac{mc}{e\tau_b}\frac{\partial J}{\partial \psi}, \tag{3}$$

where $\Delta\phi$ is the net change in toroidal angle ϕ over one bounce period and τ_b is the bounce period. By differentiation of Eq. (2), $\partial J/\partial\psi$ is found to have three components corresponding to the ∇B drift, the curvature drift and a shear term. The ∇B drift contributes more strongly than the curvature drift for the trapped particles because $v_{\|}^2 < v_{\perp}^2$. Particles trapped on the outboard side of the torus have a ∇B drift in the unstable direction, at least up to moderate β values. Kadomtsev and Pogutse[9] have shown that positive shear (tokamak-like) is destabilizing for the collisionless trapped particle mode, while negative shear is stabilizing.

The collisionless trapped particle regime would be difficult to achieve in tokamak operation; more likely is the trapped electron mode regime. For $\nu_* < 1$, the single particle drifts still influence stability. This effect was considered by Adam, Tang and Rutherford.[10] They solved the dispersion relation

$$\left[1 + \tau - \left(\tau + \frac{\omega_*}{\omega}\right)\Gamma_0 - \eta_i \frac{\omega_*}{\omega} b\,(\Gamma_1 - \Gamma_0)\right]\phi = \left\langle \frac{\{\omega - \omega_*\,[1 + \eta_e\,(\epsilon/T_e - 3/2)]\}\bar{\phi}}{\omega - \omega_d + \iota\hat{\nu}\,(\epsilon/T_e)^{-3/2}} \right\rangle, \tag{4}$$

where $\bar{\phi}$ is the bounce average of the potential, $\langle A\rangle$ denotes the velocity-space average of A over trapped particles, ω_d is the bounce average of the electron drift frequency, $\hat{\nu}$ is the effective electron collision frequency, and the other quantities which are not considered here are defined in Ref. 10. Their results show that the growth rate is reduced significantly by setting ω_d equal to zero—by 25% at $\nu_* = 0.5$ and by a factor of 3 at $\nu_* = 0.1$. Expanding the trapped particle velocity integrals for $\omega_d < \omega$, $\nu_{e,\text{eff}}$, the lowest order drift term is proportional to $\langle\omega_d\rangle$. Thus our goal for shape optimization is the reduction or reversal of $\langle\partial J/\partial\psi\rangle_{\text{trapped}}$ over all flux surfaces.

The extension of the dissipative trapped electron mode to lower frequency is the dissipative trapped ion mode[8] with $\nu_{i,\text{eff}} < \omega < \nu_{e,\text{eff}}$; here $\nu_{i,\text{eff}}$ is the effective trapped ion collision frequency. In this case it has been shown that drift reversal of the bounce-averaged ion drift frequency can have a significant stabilizing effect.[8]

To determine an optimal shape we began with a fixed boundary equilibrium code[11] and parameterized the outer boundary by a fourth order polynomial in x and y with six shape coefficients, C_i, to be determined. The equilibrium code requires a specification of $q(\psi)$ and $p'(\psi)$ to compute an equilibrium. We began with $p' = 0$ and $q(\psi) = q_{\text{axis}} + (q_{\text{lim}} - q_{\text{axis}})\tilde{\psi}^{\alpha_q}$ where $q_{\text{axis}} = 1.05$, $q_{\text{lim}} = 4.1$, $\alpha_q = 2.5$, and $\tilde{\psi}$ is a normalized ψ, ranging from 0 at the axis to 1 at the boundary. With simple circular and inverse "dee" shapes we quickly established numerically that decreasing R/a decreased $\langle\partial J/\partial\psi\rangle$ as desired. Therefore we chose an extreme example of $R/a = 1.25$ with which to perform the shape optimization.

The shape optimization was carried out automatically by a computer program which: (1) calculates the n^{th} equilibrium; (2) evaluates $\gamma_n = \Sigma_{i=20}^{40} \langle \partial J/\partial \psi \rangle_i$ where i is a flux surface index and $i = 41$ is the limiter surface; (3) if $\gamma_n < \gamma_{n-1}$ then it keeps the equilibrium n; (4) makes an incremental change to one of the shape parameters C_i; and (5) return to (1).

Using this procedure we obtained the optimal shape shown in Fig. 1. Depending upon the initial shape, the code tends to reduce the height-to-width ratio. For the case in Fig. 1, we held the height-to-width ratio fixed at 1:2. With this shape and $\beta = 0$ we achieved drift reversal on the outer 50% of the flux surfaces using poloidal flux as a flux surface label. This shape is very similar to that suggested by Ohkawa[1] to ensure that most trapped particles are in a "good" curvature region.

The equilibrium just described has a large edge current density, particularly on the inboard side. This arises because we have set $q_{\text{lim}} = 4$ while the shape has evolved to one having an x-point just outside the plasma. To eliminate the edge current density we used the free boundary equilibrium code GAEQ[12] and specified ff' instead of q.

The free boundary calculations used 32 external coils to produce the comet shape. The comet configuration is easy to generate and has a robust equilibrium solution space. The profiles p' and ff' are

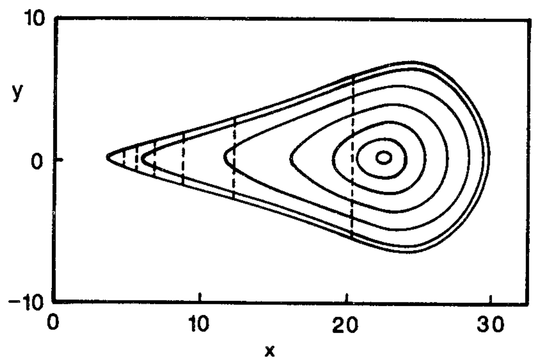

FIGURE 1 Flux surface (solid lines) and mod B (dashed lines) contours for comet equilibrium. Outer boundary is given by $C = x^2 + 4y^2 + 0.375x^3 - 4.85\, xy^2 + 0.0x^4 + 3.35x^2y^2 - 0.5y^4$.

given by

$$p' = \frac{j_N \beta_p}{c R_0} \left[\exp\left(1 - \tilde{\psi}^{\alpha_p}\right) - 1 \right] \tag{5}$$

and

$$ff' = \frac{4\pi R_0 j_N}{c} (1 - \beta_p) \left[\exp(1 - \tilde{\psi}^{\alpha_f}) - 1 \right], \tag{6}$$

where j_N is a normalization constant used to set the total plasma current, R_0 is a constant toroidal radius, and α_p, α_f, and β_p are the parameters which define the current profile.

The drift reversal results for a sequence of comet equilibria with $\beta = 0$ and $\alpha_f = 40$ are shown in Fig. 2. The percentage of poloidal flux surfaces with drift reversal is plotted as a function of the safety factor on axis, q_{axis}. The drift reversal occurs first on the outermost flux surfaces and works its way towards the magnetic axis as q_{axis} increases. The increase in drift reversal as q_{axis} is raised is due to the reduced paramagnetic effect of the current. At $\beta = 0$ the paramagnetic effect raises B in the plasma and thus worsens the

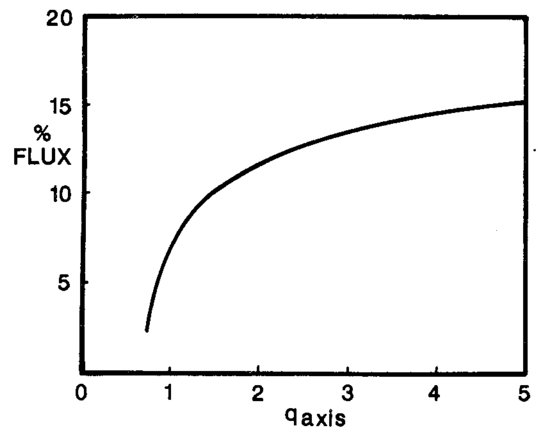

FIGURE 2 Percentage of flux surfaces with drift reversal versus q_{axis}. $\beta = 0$ and $\alpha_f = 40$.

effect of the ∇B drifts on the outboard region of the plasma. As β is increased the drift reversal improves, in part due to the diamagnetic effect on the ∇B drift.

Shown in Fig. 3 is the ballooning mode stability boundary and the contours of constant $\langle \partial J/\partial\psi \rangle$ reversal as β_p and the current half-width are varied. Drift reversal occurs on the outermost flux surfaces and thus drift reversal on 10% of the flux surfaces could provide a significant insulating layer. The marginal ballooning mode stable line almost coincides with the contour of $\beta = 3.1\%$. These equilibria have $q_{\text{axis}} = 1.005$ while the Mercier stability criterion for these configurations generally demand only $q_{\text{axis}} \gtrsim 0.75$. Therefore, these do not represent optimal ballooning mode stable plasma configurations. Note that the drift reversal contours are skewed with respect to the ballooning mode stability boundary. This indicates that substantial improvement may be possible by using different profiles to improve either drift reversal or stable β while holding the other nearly constant. One may also choose to change the shape as β is increased to improve the ballooning stability.

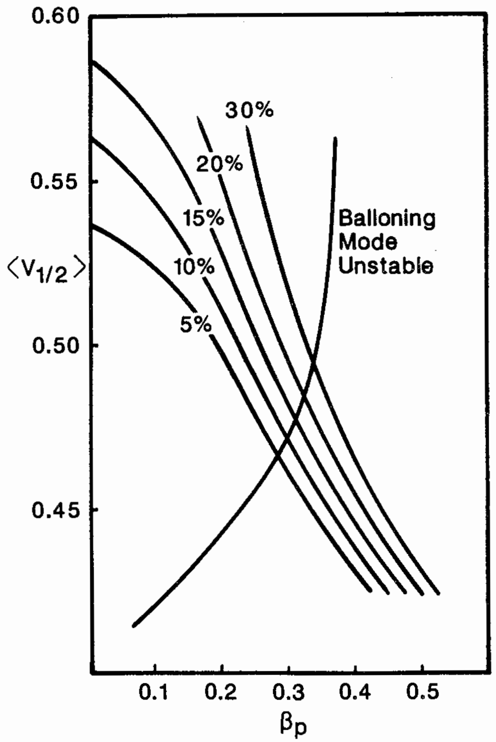

FIGURE 3 Ballooning mode stability boundary and contours of percentage of flux surfaces with drift reversal. $V_{1/2}$ is the fraction of plasma volume containing half of the toroidal current.

It is of interest to compare the above results to those of a more conventional "dee"-shaped equilibrium with $R/a = 1.5$ and height-to-width ratio 1.5. In this case we were able to achieve drift reversal only at significant values of β—above the ballooning mode limit unless $q_{\text{lim}} \lesssim 2.5$. The primary difference between the comet and conventional equilibria is that the comet can achieve drift reversal at $\beta = 0$.

If anomalous transport is due primarily to trapped particle modes, drift reversal could indicate a reduction in transport coefficients by as much as an order of magnitude or more if $\nu_* < 0.5$. Furthermore, $\nu_* = \nu/\omega_b\epsilon^{3/2}$ is reduced in the comet due to the large value of ϵ, 0.8 at the plasma boundary. This large value of ϵ leaves little room for coils to drive the ohmic current, so some other means of current drive may be required. Larger values of R/a need to be explored as well as a means of improving the stable β ballooning limit. Although low n stability to ideal MHD modes was not studied, it is assumed that these modes can be wall stabilized in the same way as for vertically elongated tokamaks.

Because the comet can achieve drift reversal at $\beta = 0$ it could provide an important experimental test to determine if trapped particle modes contribute to tokamak transport.

R. L. MILLER, M. S. CHU,
R. R. DOMINGUEZ and T. OHKAWA
General Atomics,
San Diego, California 92138

Received October 6, 1988

References

1. T. Ohkawa, General Atomics Rep. GA-A19184 (1988), submitted to Kakuyugo Kenkyu.
2. R. D. Stambaugh, R. W. Moore, L. C. Bernard, A. G. Kellman, E. J. Strait

et al., in *Plasma Physics and Controlled Nuclear Fusion Research* (Proc. 10th Int. Conf. London, 1984) (IAEA, Vienna, 1985), Vol. 1, p. 21.
3. K. McGuire, P. Beirsdorfer, M. Bell, K. Bol, D. Boyd *et al.*, *ibid.*, Vol. 1, p. 117.
4. F. Troyon, R. Gruber, H. Saurenmann, S. Semenzato and S. Sulci, Plasma Phys. Contr. Fusion **26**, 209 (1984).
5. M. Okabayashi and R. Freeman, Phys. Fluids **15**, 359 (1972).
6. A. H. Glasser, E. A. Frieman and S. Yoshikawa, Phys. Fluids **17**, 181 (1974).
7. D. R. Dobrott and J. M. Greene, Plasma Phys. **17**, 929 (1975).
8. W. M. Tang, Phys. Fluids **17**, 1249 (1974).
9. B. B. Kadomtsev and O. P. Pogutse, Nucl. Fusion **11**, 67 (1971).
10. J. C. Adam, W. M. Tang and P. H. Rutherford, Phys. Fluids **19**, 561 (1976).
11. R. L. Miller and J. W. VanDam, Nucl. Fusion **27**, 2101 (1987).
12. F. J. Helton and T. S. Wang, Nucl. Fusion **18**, 1523 (1978).

A Choice of Magnetic Configuration of Torsatron/Heliotron Devices Based on Max⟨I⟩ and Max⟨J⟩

A designing method to improve the plasma confinement in torsatron/heliotron devices is proposed. In order to reduce the direct orbit loss and the associated neoclassical transports, the condition of Max⟨I⟩, which corresponds to minimizing the shift of the drift orbit from the magnetic surface, is required. The concept of Max⟨J⟩ is combined to reduce the anomalous transport due to the toroidally trapped particle modes. This can be done by tailoring the toroidal and helical ripples by external multipole components with the aid of the winding law of helical coils. Desired ripple profiles impose the constraints for the machine parameters.

Key Words: *helical device, configuration, trapped particles, ripples, transport improvement*

1. INTRODUCTION

There are varieties of magnetic configuration of helical systems in thermonuclear fusion research. In comparison with a tokamak device, such varieties may give us the freedom to choose the better (best) configuration. Since the choice imposes the constraints on the other freedoms, it requires profound study. The logical method of how we make the choice has not yet been established.

In a previous report,[1] we considered perspectives on low-aspect-ratio torsatron/heliotron system based on the present data bases of MHD, transport, particle control and boundary plasma control, plasma production and heating and improved confinement char-

Comments Plasma Phys. Controlled Fusion
1989, Vol. 12, No. 3, pp. 133–139
Reprints available directly from the publisher
Photocopying permitted by license only